

## Calculation of the magnetic states of cobalt overlayers on copper (111)

R. H. Victora and L. M. Falicov

*Materials and Molecular Research Division, Lawrence Berkeley Laboratory and Department of Physics,  
University of California, Berkeley, California 94720*

(Received 9 May 1983)

One- and two-atom layers of cobalt on a copper (111) surface were found to be magnetic with a spin polarization close to the bulk value. The calculation was performed in a tight-binding scheme, with single-site, full orbital interactions treated self-consistently. Antiferromagnetic and ferrimagnetic states with a two-atom periodicity were examined. A new type of "spatially modulated" state was found. The density of states and the spatial distribution of magnetization were obtained for each configuration. The ferromagnetic state was found to have the lowest total energy; the energy of the spatially modulated state was, however, calculated to be only 0.03 Ry per surface atom higher. Agreement with photoemission experiments is satisfactory: It is excellent for a one-atom layer of Co on Cu (111), but a theoretically predicted shift in peak location with Co layer thickness is not found experimentally. Calculations for both pure Cu (111) and Co on Cu (111) show that the spectral features observed at the corner of the surface Brillouin zone arise from the totally symmetric electronic states.

## I. INTRODUCTION

Recently, there has been renewed interest in the magnetism and related properties of thin magnetic transition-metal layers deposited on nonmagnetic substrates. These metals (Fe,Co,Ni) are itinerant ferromagnets; that is, their magnetization derives from the spin polarization of the itinerant  $d$  electrons. In crossing the Periodic Table from Fe to Ni, there is an increase in the number of these  $d$  electrons and an accompanying decrease in the  $d$  band widths. The diminishing number of  $d$  holes is associated with a drop in the bulk magnetization<sup>1</sup> per atom from 2.22 Bohr magnetons per atom in Fe, to 1.72 in Co and 0.61 in Ni. The magnetic properties also greatly depend on the electronic structure because the  $d$  electrons are very sensitive to local environment. Consequently, differing substrates, overlayers, and structure of the interface yield a large variety of observed phenomena.

Experimental evidence shows that two layers of Ni on Cu form a magnetic system,<sup>2,3</sup> but Ni on a Pb-Bi alloy substrate or on an Al substrate is paramagnetic below 2.5–3 atomic layers.<sup>4,5</sup> However, Co and Fe retained their magnetic moment on these same substrates, even when deposited in subatomic layers.<sup>4,5</sup> Theoretical investigation shows that one layer of Ni on Cu(100) is substantially magnetic,<sup>6,7</sup> while the same system on the (111) surface is not.<sup>7</sup> It is also found both theoretically<sup>7,8</sup> and experimentally<sup>2,9</sup> that the surface layer of a magnetic metal is magnetic. In addition, (hypothetical) unsupported monolayer films are theoretically found to have even greater magnetization than bulk.<sup>7,10</sup> This suggests that the reduction in magnetism for thin films on nonmagnetic substrates is caused by the substrate and not by the free surface. In fact, it is believed<sup>7</sup> that the crucial mechanism acting to suppress Ni magnetization at the Ni-Cu interface is hybridization of the Ni  $d$  band with the Cu  $sp$  band, which changes the shape of the band edge and

reduces the "effective" number of  $d$  holes. Both Fe and Co, which have many more holes, should be relatively immune to this effect.

The particular system addressed in this work [Co on Cu(111)] has also been studied previously. Gonzalez *et al.*<sup>11</sup> and Miranda *et al.*<sup>12,13</sup> used angle-resolved photoemission spectroscopy to determine a surface density of states for one and two layers of Co deposited on a clean, well-ordered Cu(111) surface. Observations at the surface Brillouin-zone center produced several large peaks, one of which is near the Fermi energy and thus not normally associated with the Cu density of states (DOS). The similarity between this peak and a bulk Co DOS, interpreted as ferromagnetic by Himpsel and Eastman,<sup>14</sup> suggested to them that Co is magnetic with an exchange splitting of 0.7 eV at the  $\bar{\Gamma}$  point of the surface Brillouin zone. The system was also examined theoretically<sup>11</sup> with the use of a tight-binding Hamiltonian with a rigid exchange band approximation. The magnetization was constrained to equal the bulk Co magnetization, and local charge neutrality was required. The resultant low exchange splitting (0.7 eV) produced a cobalt DOS with three peaks near the Fermi energy, superposed on a normal Cu background. Several very weak structures near the main experimental Co peak are interpreted as support for the ferromagnetism of this system.

Several related systems have also been examined. Mössbauer spectroscopy shows that two and four layers of Co are magnetic when epitaxially grown on Cu(111) surfaces.<sup>15</sup> Both theoretical and experimental investigations<sup>11</sup> provide evidence for the ferromagnetism of a Co overlayer on a Cu(100) surface, but this time accompanied by a  $c(2 \times 2)$  reconstruction. This is interpreted as being caused by ferromagnetically induced charge-density waves.

In this paper we present results of calculations for the magnetic and electronic properties of thin (one- and two-

layer) Co films deposited on the Cu(111) surface. We use the Slater-Koster parametrized tight-binding scheme in which the one- and two-center integrals are fitted to the bulk band structure. The exchange interaction is treated self-consistently in a single-site approximation. This scheme has been previously used and produced excellent agreement with both experiment and state-of-the-art calculations. A Green's-function transfer-matrix method allows for representation of the infinite Cu bulk. A two-atom surface cell permits possible breaking of spatial symmetry such as antiferromagnetism, ferrimagnetism, etc. The total energy of various configurations is evaluated. It is to be emphasized that our technique allows for breaking of the rigid-band approximation, if self-consistency should demand it.

## II. CALCULATION

This section describes our calculations. Sections IIA and IIB describe the Hamiltonian and our method of evaluation, respectively. Section IIIC describes the numerical accuracy of our work and the possible errors introduced by our major approximations.

### A. The Hamiltonian

We take our Hamiltonian to be the sum of a one-electron term  $H_0$  and an electron-electron interaction term  $H_{e-e}$ . For  $H_0$  we choose the parametrized tight-binding scheme of Slater and Koster.<sup>16</sup> The Hamiltonian  $H_0$  is written in terms of one- and two-center integrals, which are treated as parameters chosen to fit the bulk bands structure. In Co (as in Ni) there is a marked discrepancy between the calculated and the experimentally measured bandwidth (photoemission experiments). We have chosen the calculated paramagnetic band structure of Moruzzi *et al.*,<sup>17</sup> with the belief that discrepancies with photoemission data are caused by additional many-body effects, as has been argued<sup>18,19</sup> for Ni. We include  $s$ ,  $p$ , and  $d$  orbitals, with interactions up to second-nearest neighbors. For the matrix elements between Co and Cu, we take the geometric mean of the respective Co-Co and Cu-Cu matrix elements. For three of the second-nearest neighbor elements, the Co-Co element has the opposite sign of the Cu-Cu element. In this case we use the arithmetic mean. The two sets of intersite matrix elements are similar, so the results are insensitive to the precise scheme for choosing the Co-Cu matrix elements.

For the electron-electron interaction we use a single-site approximation which has been extensively discussed,<sup>20</sup>

$$H_{e-e} = \sum_{i,\sigma,\sigma'} \sum_{\alpha,\beta,\gamma,\delta} U_{\alpha\beta\gamma\delta} c_{i\alpha\sigma}^\dagger c_{i\beta\sigma'}^\dagger c_{i\gamma\sigma} c_{i\delta\sigma}, \quad (1)$$

where  $c_{i\alpha\sigma}^\dagger$  creates an orbital of symmetry  $\alpha$  and spin  $\sigma$  at site  $i$ .

We treat  $H_{e-e}$  in the Hartree-Fock approach; we can, with some approximations, reduce  $H_{e-e}$  to a simple form for the on-site potential shifts,

$$\begin{aligned} \Delta E_{d\nu\sigma} &= -\frac{1}{2}(U-J)\langle m_{d\nu\sigma} \rangle - \frac{1}{2}J\langle m_{d\sigma} \rangle \\ &\quad + \frac{1}{2}(U-2U'+J)\langle n_{d\nu} - n_{d\nu}^0 \rangle \\ &\quad + V_{sd}\langle n_s - n_s^0 \rangle + V_{dd}\langle n_d - n_d^0 \rangle, \\ \Delta E_{s\sigma} &= V_{ss}\langle n_s - n_s^0 \rangle + V_{sd}\langle n_d - n_d^0 \rangle. \end{aligned} \quad (2)$$

Here  $\Delta E_{d\nu\sigma}$  is the on-site potential shift for a  $d$  orbital of symmetry  $\nu$  and spin  $\sigma$ , measured relative to the value for the pure paramagnetic metal. By  $m_{d\nu\sigma}$  we denote the spin polarization ( $n_{d\nu\sigma} - n_{d\nu\bar{\sigma}}$ ) in the  $d$  orbital of symmetry  $\nu$  at a given site, and  $m_{d\sigma} \equiv \sum_{\nu} m_{d\nu\sigma}$ . The total  $d$  occupancy at the site is denoted by  $n_d \equiv \sum_{\nu,\sigma} n_{d\nu\sigma}$ , and the value for the respective pure metal is  $n_d^0$ . Quantities for  $s$  and  $p$  orbitals are similarly defined. In (2),  $s$  refers to the entire  $sp$  complex.

We define  $U$  as the on-site direct Coulomb integral between  $d$  orbitals of the same symmetry (rescaled by correlation effects; see below),  $U'$  is the integral between  $d$  orbitals of different symmetry, and  $J$  is the exchange integral. We define  $V_{dd} \equiv U' - \frac{1}{2}J$ , which gives the effective (repulsive) interaction between  $d$  electrons, aside from magnetic effects. We similarly define an effective interaction  $V_{ss}$  among  $sp$  electrons, and  $V_{sd}$  between  $sp$  and  $d$  electrons. We neglect the on-site exchange integrals other than between  $d$  orbitals. The ratios  $U:U':J$  are taken to be 5:3:1 as suggested by Herring.<sup>21</sup> Similar results are obtained for the ratios suggested by other estimations<sup>22,23</sup> as long as the absolute magnitude is scaled to give the correct bulk Co magnetization,  $\mu = 1.72\mu_B$ . Such scaling is necessary in any case when we work in the Hartree-Fock approximation, since the effective interaction is reduced by correlation effects.<sup>20</sup>

It is difficult within the tight-binding approximation to treat charge transfer accurately at the surface. To avoid this problem and still treat charge transfer and potential shifts at the surface in a simple way, we impose upon our potential the constraint

$$\Delta n_{sp} = \Delta n_d = 0. \quad (3)$$

That is, the average on-site potentials of the  $d$  orbitals and of the  $s$  and  $p$  orbitals are fixed by the requirement that the total occupancies of the  $sp$  and  $d$  complexes at any site not differ from the bulk values. More fully self-consistent calculations<sup>8,10</sup> suggest a transfer of about 0.1 electrons per atom from the  $sp$  band to the  $d$  band at the surface. By neglecting this, we may expect to exaggerate the surface magnetization by roughly  $0.1\mu_B$  per atom, an acceptable level of error.

### B. Method of evaluation

Our calculation uses a Green's-function transfer-matrix method to represent the Co overlayers on the semi-infinite bulk Cu crystal. This scheme treats most of the infinite number of substrate layers as unaltered bulk Cu atoms, with only a finite number of layers near the surface treated self-consistently. A more detailed description of this method is provided elsewhere.<sup>7</sup>

The one-atom hexagonal unit surface cell is shown in Fig. 1(a). A single unsupported Co monolayer would have

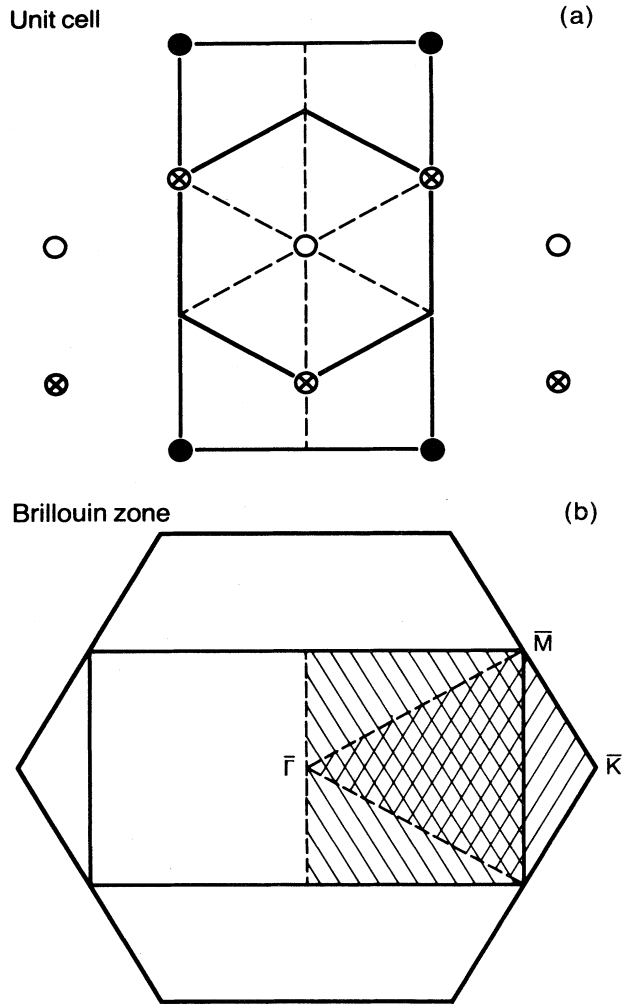


FIG. 1. (a) One- and two-atom surface unit cells used in the calculations. Open and closed circles represent the Co surface-layer atoms. Crossed circles are the Cu atoms in the adjacent layer. Dashed lines denote reflection planes. (b) Surface Brillouin zones for the unit cells of (a). Symmetry points are indicated. The hatching shows the irreducible parts of the rectangular and hexagonal cells.

symmetry  $C_{6v}$ ; however, the presence of the Cu substrate reduces the symmetry to  $C_{3v}$ . The hexagonal Brillouin zone with its irreducible ( $\frac{1}{6}$ ) wedge is shown in Fig. 1(b). Table I lists the character table for the group  $C_{3v}$ .

The two-atom rectangular unit surface cell is also shown in Fig. 1(a). The presence of two unlike atoms leaves only the symmetry of a single vertical reflection plane. The corresponding rectangular Brillouin zone is half the size of the one-atom hexagonal Brillouin zone [Fig. 1(b)]. Note that it divides into only two irreducible (rectangular) parts.

The search for a self-consistent solution was begun at a variety of starting points and thus a large portion of variational parameter space has been mapped. Nevertheless, it is entirely possible that, within our ten-dimensional space (five  $d$  orbitals, two spin polarizations per atom), we may

TABLE I. Character table for point group  $C_{3v}$ .

	$E$	$2C_3$	$3\sigma_v$
$\Lambda_1$	1	1	1
$\Lambda_2$	1	1	-1
$\Lambda_3$	2	-1	0

have missed one or more self-consistent solutions. It is unlikely, however, that the lowest-energy state would be missed by our procedure.

We calculated the total energy of each self-consistent state using the well-known formula<sup>24</sup>

$$E = \sum_{n, \vec{k}} \left( \epsilon_{\vec{k}} - \frac{1}{2} \sum_{n', \vec{k}'} H_{e-e} \right), \quad (4)$$

where  $\epsilon_{\vec{k}}$  is the one-particle removal energy and the sums are performed over the occupied states. The nonintuitive term involving  $H_{e-e}$  corrects for the double counting of the electron-electron interaction.

### C. Accuracy

Here we discuss first the numerical accuracy of our calculations and second, the crucial approximations in our Hamiltonian and their effect on the reliability of the model.

Convergence of our calculation is required in the summations of both the energy and wave-vector variables. The energy integration consists of 48 points chosen along a complex contour with the aid of the method of Gaussian quadratures.<sup>25</sup> Our criterion for achieved self-consistency of the potentials is set equal to the estimated accuracy of our integration: 0.01 electrons. For calculations involving a two-atom unit surface cell, reasons of economy demanded a slightly less accurate 24-point integration.

Convergence with respect to wave-vector sample is provided by 12 wave-vectors evenly distributed throughout the irreducible two-atom rectangular half-cell. This corresponds to 24 wave vectors in the one-atom irreducible wedge. We also experimented with specially chosen wave-vector samples to help ensure that our two-atom states were not some unwanted consequence of the wave vectors chosen.

We now recapitulate the most crucial approximations in our Hamiltonian, and consider their effects. The most obvious approximation here is (3), in which the self-consistent change in the potential is approximated by an on-site term, determined by imposing a zero-charge-transfer condition on the  $sp$ - and  $d$ -projected subbands separately at each site. Comparison with fully self-consistent calculations<sup>10,26</sup> suggests that this is an excellent approximation. Still, the uncertainty of up to 0.1 electron in the local  $d$  occupancy corresponds to a possible error of up to  $0.1\mu_B$ , which may be measurable for Co systems. However, there is no evidence that any available methods are accurate to better than  $0.1\mu_B$  for inhomogeneous systems in any case. Approximation (3) also neglects the crystal-field splitting of the on-site potential.

Our Hartree-Fock treatment necessarily exaggerates the

exchange splitting, which is reduced by correlation effects. This is not a serious problem in the calculation of the magnetization since the majority band would be significantly below the Fermi energy in any case. However, it may distort the DOS and make comparison with photoemission experiments somewhat difficult.

The use of a tight-binding Hamiltonian should be analyzed with care. This method provides a rather good treatment of the  $d$  band, but the handling of the  $sp$  band is less accurate. Since  $sp-d$  hybridization plays an important role here, the tight-binding approximation introduces some risk of reduced quantitative accuracy.

Finally, it is important to note that, if many-body effects are important, the one-electron DOS which we calculate may not be the same as the excitation spectrum which is measured by photoemission. In particular, bulk Co and Ni exhibit a compressed photoionization spectrum<sup>14,27,28</sup> compared to calculated DOS. Since the Fermi energy is fixed, it is the lowest-energy peaks which experience the largest displacement. In the Co on Cu(111) system, this effect is probably reduced due to the considerable hybridization of the majority Co peaks with the Cu  $d$  bands as well as normal  $sp-d$  hybridization. Nonetheless, substantial deviations between calculated and measured band structures are possible, particularly at the lower energies.

Ultimately, we must base our assessment of overall accuracy upon comparison with reported results of fully self-consistent calculations for simple systems, and with experiment. Such comparisons are few, but they suggest that our methods reliably predict the quantitative magnetization of heterogeneous systems.<sup>7</sup> Other important conclusions which we draw either involve comparisons of different systems, in which case our errors should approximately cancel, or appear to be model independent.

### III. RESULTS

In this section we discuss the results of our calculation and compare them with the photoemission experiment of Miranda and co-workers.<sup>11-13</sup> Section III A discusses our preliminary calculation of the clean Cu(111) surface. Other sections consider the combined Co on Cu system employing a one-atom (Sec. III B) and two-atom (Sec. III C) unit surface cell.

#### A. Clean Cu(111) surface

As an aid to the interpretation of the Co on Cu(111) experiments, Miranda and co-workers<sup>11-13</sup> first examined the angle-resolved density of states for a clean Cu(111) surface. Of special interest is the off-normal measurement made at the  $\bar{K}$  point in which a sharp narrow peak was observed at 0.16 Ry below the Fermi energy. Seeking to understand the nature of this unusual peak before attempting the more complicated Co-on-Cu system, we performed a preliminary calculation for the Cu(111) surface. We compared our results for the total DOS with the calculation of Appelbaum and Hamann<sup>29</sup> and found the *maximum* disagreement on peak location to be 0.02 Ry. This can be taken as some indication of our accuracy with respect to surface effects.

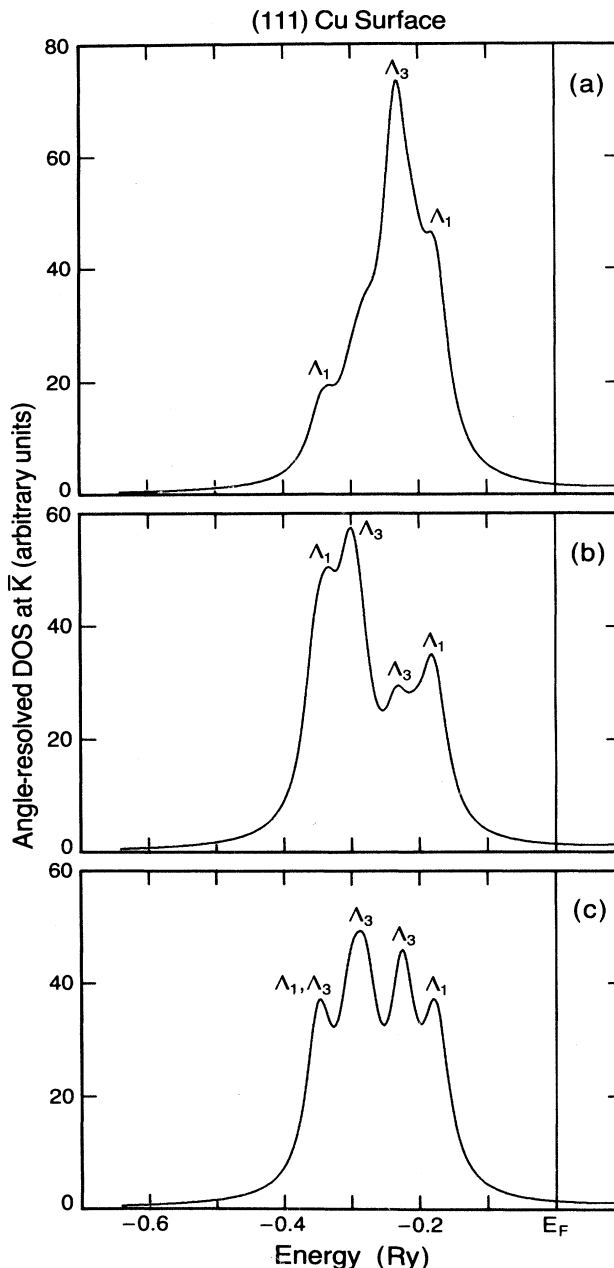


FIG. 2. Projected density of states for an ideal Cu(111) surface at the  $\bar{K}$  point of the surface Brillouin zone. (a) Surface layer; (b) second layer; (c) third layer (not self-consistent). Curves include a Lorentzian broadening of halfwidth 0.022 Ry at half maximum. The peaks are labeled according to symmetry.

Figure 2 shows the layer-projected angle-resolved DOS at the  $\bar{K}$  point. The symmetry at this point is the same as for the whole surface ( $C_{3v}$ ), which permits the continued use of the familiar  $\Lambda_1, \Lambda_2, \Lambda_3$  labels. The normal selection rule for  $s$ -polarized light, i.e., only states of symmetry  $\Lambda_3$  measured, fails here because the final state is at an angle from the surface normal and thus does not have  $C_{3v}$  symmetry. We find that a bulklike peak of symmetry  $\Lambda_1$  falls

TABLE II. Spin polarization and splitting by orbital for one layer Co on Cu(111).

Bulk symmetry		$t_{2g}$	$e_g$
Degeneracy		3	2
Surface symmetry	$\Lambda_1$		$\Lambda_3$
Degeneracy	1	2	2
Radial wave function	$xy + yz + zx$	$2xy - yz - zx;$ $yz - zx$	$2z^2 - x^2 - y^2$ $x^2 - y^2$
Spin polarization	0.14	0.36	0.41
Splitting at zone center <sup>a</sup>	0.210 Ry	0.246 Ry	0.234 Ry

<sup>a</sup>Mixing occurs between all  $\Lambda_3$  states and between the  $d$  orbital of symmetry  $\Lambda_1$  and the  $sp$  orbitals. Those peaks which contain the largest contribution from a particular column are used to generate the splitting value.

very near the experimental peak location, while no other peak is within the error bars stated earlier. Thus the peak is clearly identified and comparisons can be made with the Co-Cu system.

#### B. Co on Cu(111): One-atom surface cell

Bulk Co is believed<sup>30</sup> to possess a spin polarization of 1.56. The effect of the free surface is to make the surface Co more like a free atom and hence substantially raise the spin polarization. On the other hand, the coupling of the Co atoms to the Cu substrate may be expected to produce a large decrease in the polarization. Our calculations show that for one layer Co on the Cu(111) surface, the spin polarization of the Co atom equals 1.63. However, our approximation (3) may exaggerate this polarization by approximately 0.1 which suggests that the actual spin polarization is essentially unchanged from the bulk. This is in interesting contrast to the case of Ni on the Cu(111) surface in which the Ni magnetization is greatly suppressed. Of course, there is no contradiction present since previous calculations<sup>7</sup> have shown that small changes in substrate orientation or material composition can produce large effects. This is attributable to the delicate balance between two competing effects: enhancement by the surface and suppression by the substrate hybridization.

The  $d$  orbitals of the Co layer can be classified uniquely by specifying their bulk and surface symmetries. This facilitates detailed examination of the distribution of magnetization among orbitals (Table II). One notes that the orbital of symmetry  $\Lambda_1$  has significantly less spin polarization and exchange splitting than the orbitals of symmetry  $\Lambda_3$ . This is presumably due to its geometric orientation perpendicular to the (111) plane, which means that it points directly into the Cu substrate. In addition, its symmetry is the same as most of the Cu  $sp$  electrons, which facilitates hybridization. One interesting conclusion to be drawn from Table II is that rigid-band exchange splitting is only approximately obeyed in this Co on Cu(111) system. This contrasts to the bulk system, where our calculations found only negligible (less than 1%) exchange-splitting difference between orbitals.

We also performed our calculations for two layers of Co

on Cu(111). The top and second layers have spin polarizations of 1.65 and 1.58, respectively. The spin polarization is distributed much more evenly between orbitals although, relative to the  $\Lambda_3$  states, the  $\Lambda_1$  orbital has a slightly enhanced ( $\sim 0.06$ ) value in the surface layer and a slightly suppressed ( $\sim 0.05$ ) value in the second layer. The Cu atoms have negligible spin polarization ( $\sim 0.01$ ) independent of the number of Co overlayers.

Figure 3 shows the calculated one-electron DOS for one and two layers of Co on Cu. As in all angle-integrated DOS plots in this paper, the curves are smoothed with a Lorentzian of halfwidth 0.006 Ry at half maximum. One notes that the majority Co peaks have approximately the same energy as the Cu peaks. This leads to significant distortion of the Cu minority peaks where they hybridize with the Co.

Comparison with the experiment of Miranda and co-workers<sup>11-13</sup> is facilitated by Figs. 4 and 5. The agreement between experiment and theory for the most significant peaks of one layer Co on Cu is excellent. At the  $\bar{\Gamma}$  point, the three largest peaks coincide to within 0.01 Ry, while at the  $\bar{K}$  point the two largest calculated peaks of  $\Lambda_1$  symmetry match the experimental results to the same accuracy. The reduced contribution of the  $\Lambda_3$  states also occurred in the clean Cu(111) surface as discussed earlier, and is presumably caused by a small photoemission dipole matrix element.

The results from two layers of Co on Cu show much poorer agreement, essentially because our calculation shows the Co minority peaks shifting as the number of Co layers increases from one to two. The experiment shows no such shift. We find the discrepancy difficult to explain. Calculations of Ni on Cu show considerable differences between one and two layers of the magnetic material on the substrate. However, direct comparison is difficult because the Ni spin polarization is affected in these systems more substantially than the Co magnetization is in ours. In any case, experiment should observe band narrowing in the surface layer as is the case with the clean Cu(111) surface.

Another qualitative difficulty in comparison with the experiment of Miranda and co-workers is their observation of dispersion in the single Co layer as they change the energy of their photons. We, of course, find nondispersive peaks and are puzzled by their result.

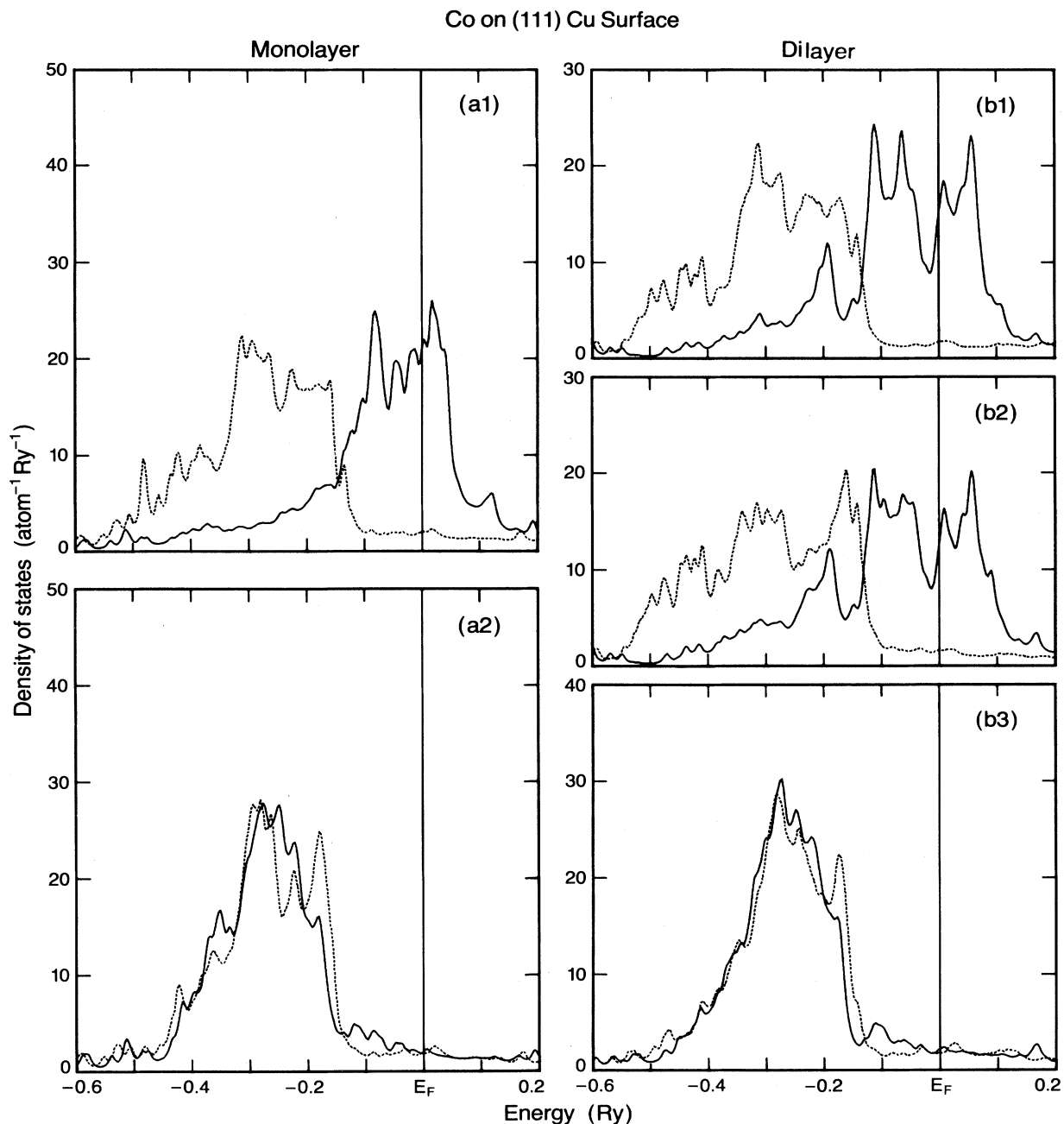


FIG. 3. Projected total density of states for the ferromagnetic state of a one- and two-atom Co layer on Cu(111). (a1) Co monolayer: Co projection. (a2) Co monolayer: Cu interface-layer projection. (b1) Co dilayer: Co surface-layer projection. (b2) Co dilayer: Co interface-layer projection. (b3) Co dilayer: Cu interface-layer projection. Solid lines are minority states; dashed lines are majority states.

### C. Co on Cu(111): Two-atom surface cell

Through the employment of the two-atom rectangular unit surface cell discussed previously, we have found three locally stable configurations for the system consisting of one layer of Co on Cu(111). The simplest of these is the ferromagnetic arrangement discussed in Sec. III B. In this state both of the atoms in the unit cell possess equal polar-

izations and are identical in all respects.

We also examine an antiferromagnetic state in which the spin polarizations of the two atoms in the unit cell have equal magnitude (1.51 per atom) but opposite orientation. Those states which possess a positive reflection symmetry are found to have the lowest spin polarization, presumably due to their hybridization with the Cu *s* states. The total energy of this configuration is found to

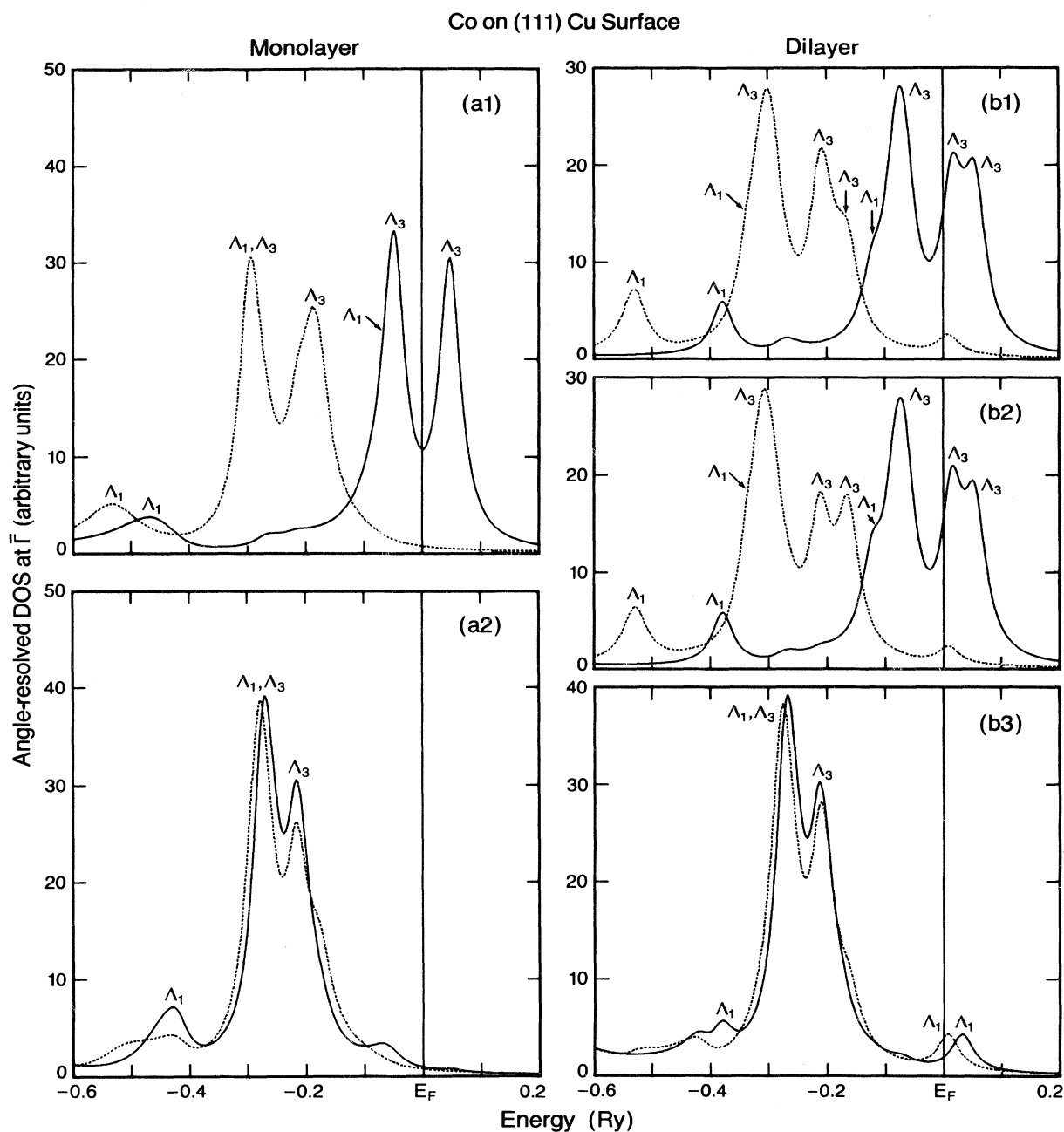


FIG. 4. Projected density of states at the  $\bar{\Gamma}$  point for the ferromagnetic state of a one- and two-atom Co layer on Cu(111). (a1) Co monolayer: Co projection. (a2) Co monolayer: Cu interface-layer projection. (b1) Co dilayer: Co surface-layer projection. (b2) Co dilayer: Co interface-layer projection. (b3) Co dilayer: Cu interface-layer projection. Solid lines are minority states; dashed lines are majority states. Curves include a Lorentzian broadening of halfwidth 0.022 Ry at half maximum. The peaks are labeled according to symmetry. Some  $\Lambda_1$  peaks are greatly obscured by the much larger  $\Lambda_3$  peaks.

be considerably higher (0.15 Ry per surface atom) than that of the ferromagnetic system, which implies that it is not the ground state.

Our third configuration is a new kind of state which we call "spatially modulated." This state possesses an approximately equal polarization of 1.60 on each atom of the unit cell, but it is distributed differently between the

orbitals. The first three orbitals, which form the  $t_{2g}$  representation in the bulk, have equal polarization on both atoms, but the last two orbitals, the " $e_g$  orbitals," switch the polarization between them as one moves from one atom to the other. This redistribution in space leads to the expression "spatially modulated." It is not to be confused with ferrimagnetic states which possess opposite and

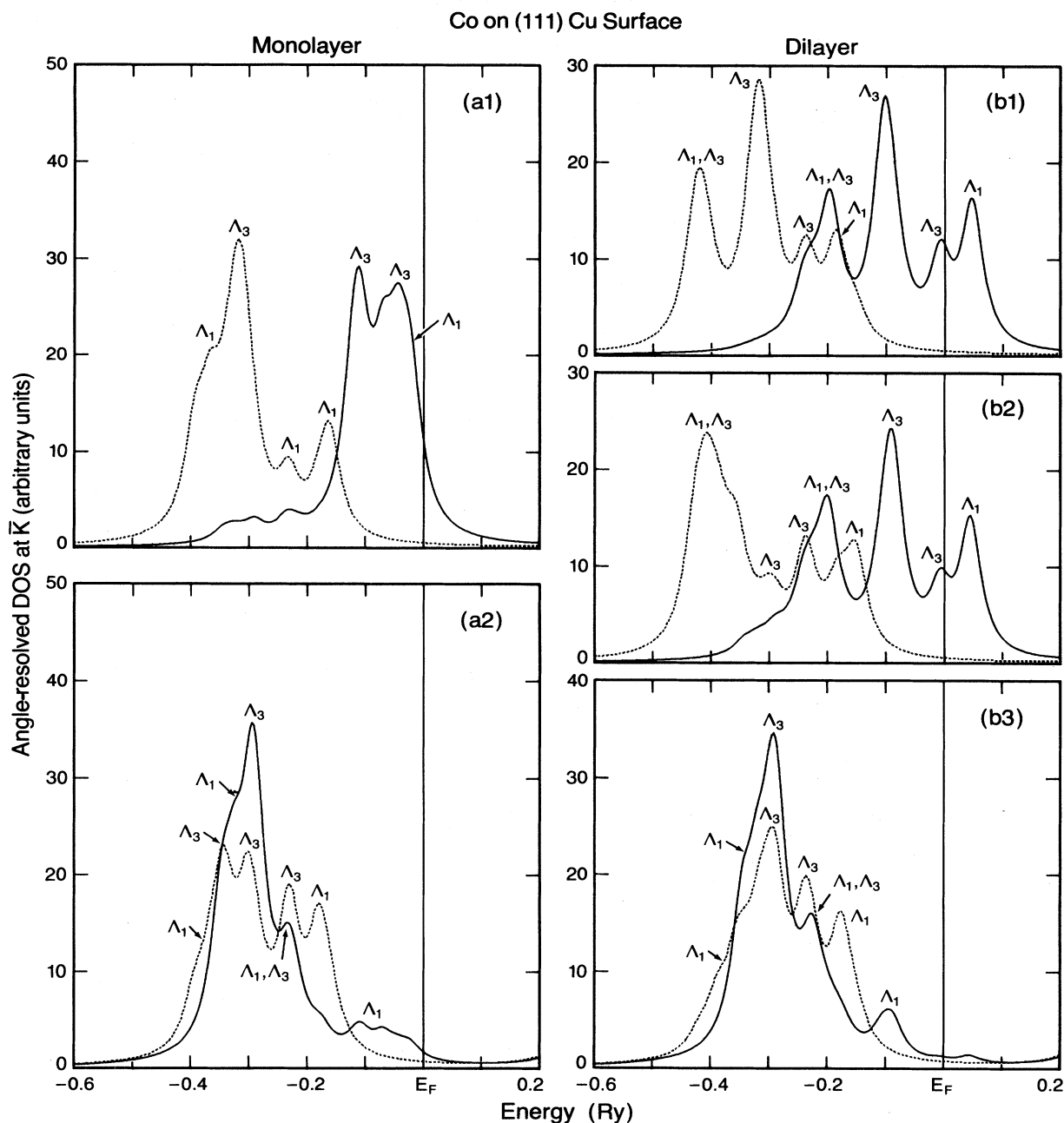


FIG. 5. Projected density of states at the  $\bar{K}$  point for the ferromagnetic state of a one- and two-atom Co layer on Cu(111). See description of Fig. 4.

unequal spins on the two atoms of the unit cell. The total energy of the spatially modulated state is calculated to be 0.03 Ry per surface atom above the ferromagnetic state. Distinctions of this small magnitude are probably not within the accuracy of our approximations. Consequently, we conclude that either the ferromagnetic or spatially modulated state could be the ground state.

Figure 6 illustrates the spatial distribution of magnetization. The plots were calculated by multiplying the spin polarization by the correct spherical harmonic and an

atomic radial function. Most trivially, the figures exhibit the  $C_{3v}$  symmetry of the ferromagnetic configuration (one reflection line is vertical, the other two at  $120^\circ$  to it) and the single vertical reflection line of the other two configurations. The wavelike modulation of the spin polarization in the antiferromagnetic case is also clearly visible. More interesting is the asymmetric accumulation of magnetization density above the middle Co atom in the spatially modulated state, leading to the concept of a small wave of periodicity equal to two atoms, superposed on a more con-



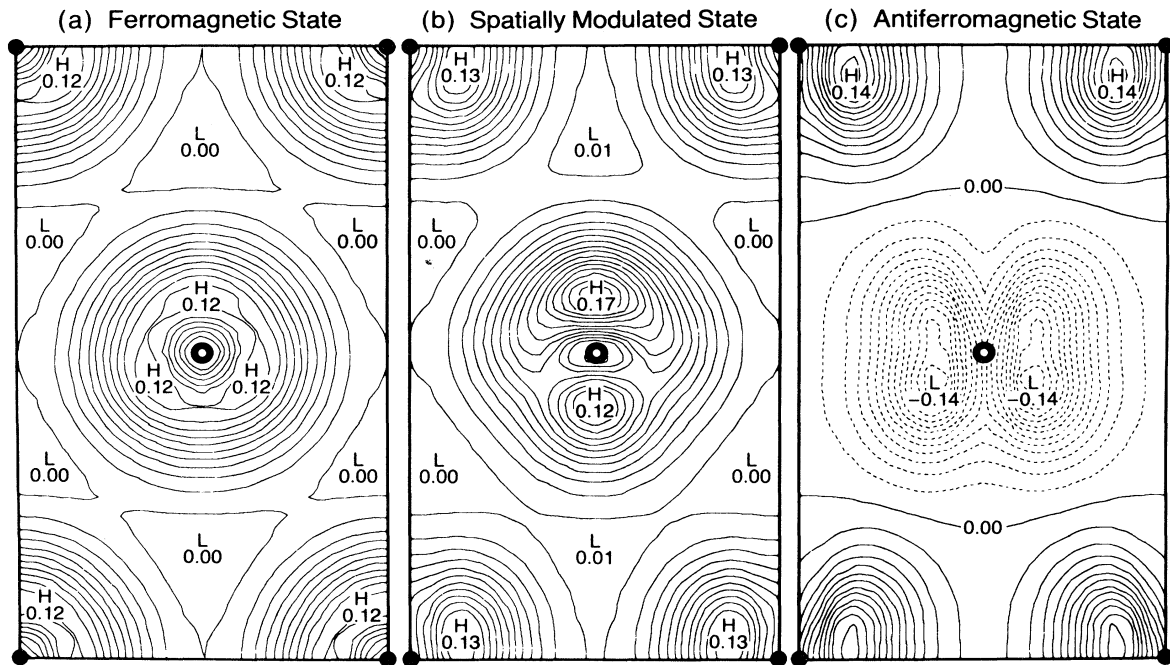


FIG. 6. Real-space magnetization density of a Co monolayer on Cu(111): the Co surface layer for (a) ferromagnetic state; (b) spatially modulated state; (c) antiferromagnetic state. Spin-up density contours are plotted in solid lines; spin-down density contours in dashed lines. All graphs are projections on the Co(111) plane of the magnetization of the "vacuum" half-space.

stant background.

Figures 7 and 8 show the total DOS for the two-atom configurations. An interesting point is that, although the spatial distribution of magnetization is quite different between the ferromagnetic and spatially modulated states, the total DOS for both spatially modulated atoms and the ferromagnetic atom are remarkably similar. Figure 9

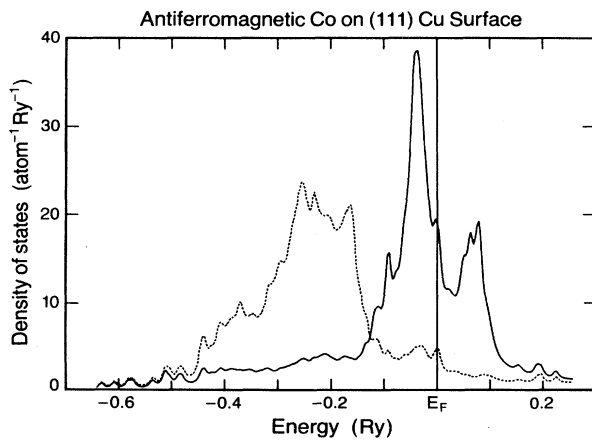


FIG. 7. Projected total density of states for the antiferromagnetic state of a Co monolayer on Cu(111) in the double cell of Fig. 1. The projection is on one of the Co atoms at the surface. (The other atom is identical if spin-up and spin-down labels are interchanged.)

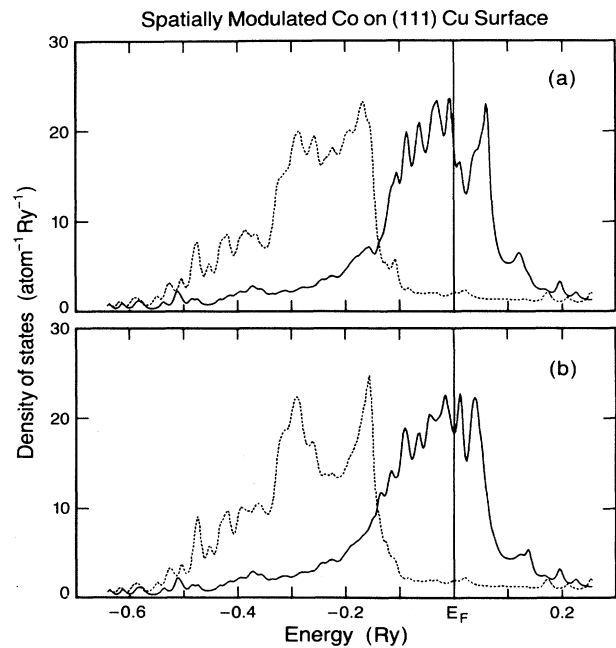


FIG. 8. Projected total density of states for the spatially modulated state of a Co monolayer on Cu(111) in the double cell of Fig. 1. (a) Projection on one of the Co atoms. (b) Projection on the other Co atom.

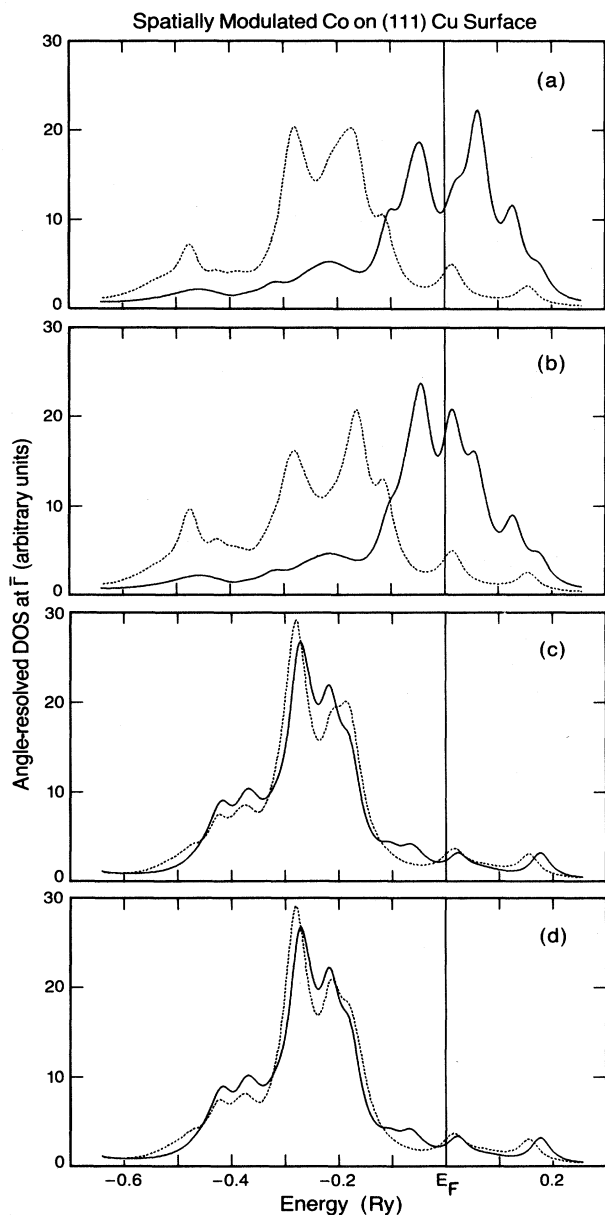


FIG. 9. Projected density of states at the  $\bar{\Gamma}$  point of the surface Brillouin zone for the spatially modulated state of a Co monolayer on Cu(111) in the double cell of Fig. 1. (a) and (b): projections on the two Co atoms. (c) and (d): projections on the two interface Cu atoms. Curves include a Lorentzian broadening of halfwidth 0.022 Ry at half maximum.

shows the angle-resolved DOS at the  $\bar{\Gamma}$  point for the spatially modulated state. Note that the symmetry breaking produces additional small peaks which may be difficult to resolve experimentally.

#### IV. CONCLUSION

One and two layers of Co on a Cu(111) surface are magnetized with a spin polarization essentially equal to the

bulk value. The rigid-band model is only approximately obeyed. The ferromagnetic state has the lowest total energy, but, within our margin of error, a spatially modulated state could be the ground state instead. The ferromagnetic, spatially modulated, and antiferromagnetic states all have approximately equal spin polarizations.

Agreement between our theory and the experiment of Miranda and co-workers is considerable, but discrepancies do exist. The quantitative correspondence between theoretical and experimental peak locations for one layer Co on Cu is excellent. The photoemission spectra at the  $\bar{K}$  point for both this system and for the clean Cu(111) surface can be consistently explained by theoretical states which transform according to  $\Lambda_1$ , the identity representation. More disappointing is the experimentally observed absence of the theoretically predicted shift in peak locations as an additional layer of Co is added. The experimentally observed displacement in Co peak location with photon energy is also puzzling, since monolayer states can have no dispersion.

Analysis of our results suggests some additional points of interest: (a) The closeness in energy between two considerably different states—ferromagnetic and spatially modulated states—indicates the presence of low-energy excitations and the likelihood of easily accessible phase transitions in the magnetic configuration of the monolayer; (b) the quantitative values of the magnetic moment in the various phases—ferromagnetic, antiferromagnetic, and spatially modulated—indicated that Co monolayers, which are itinerant magnetic systems, should behave in all respects as fairly weakly coupled localized moments of almost constant value; (c) as a consequence of (a) and (b) a fairly low Curie temperature should be expected for these systems, but there also should be persistence of the localized magnetic moment in the paramagnetic high-temperature phase.

Finally, in order to improve the comparison between our theory and photoemission experimental data, it is necessary to include in the theory the several proposed many-body effects<sup>18,19,31,32</sup> (relaxation, exciton formation, Hund rules, Auger processes) inherent in the photoemission process of highly correlated transition-metal atoms. These effects lead to band narrowing, resonant photoemission, and formation of tails and satellites.

#### ACKNOWLEDGMENTS

We wish to thank J. Tersoff for many interesting and informative conversations. We are thankful to R. Miranda and Y. Petroff for providing us with information concerning their data. This work was supported by the Director, Office of Energy Research, Office of Basic Energy Sciences, Materials Sciences Division of the U. S. Department of Energy under Contract No. DE-AC03-76SF00098.

- <sup>1</sup>C. Kittel, *Introduction to Solid State Physics*, 5th ed. (Wiley, New York, 1976), p. 465.
- <sup>2</sup>C. Rau, *Comments Solid State Phys.* **9**, 177 (1980).
- <sup>3</sup>D. T. Pierce and H. C. Siegmann, *Phys. Rev. B* **9**, 4035 (1974).
- <sup>4</sup>G. Bergmann, *Phys. Rev. Lett.* **41**, 264 (1978); *Phys. Today* **32**, (8), 25 (1979).
- <sup>5</sup>R. Merservey, P. M. Tedrow, and V. R. Kalvey, *Solid State Commun.* **36**, 969 (1980).
- <sup>6</sup>D. S. Wang, A. J. Freeman, and H. Krakauer, *Phys. Rev. B* **26**, 1340 (1982).
- <sup>7</sup>J. Tersoff and L. M. Falicov, *Phys. Rev. B* **26**, 6186 (1982).
- <sup>8</sup>C. S. Wang and A. J. Freeman, *Phys. Rev. B* **21**, 4585 (1980).
- <sup>9</sup>C. Rau and S. Eichner, *Phys. Rev. Lett.* **47**, 939 (1981).
- <sup>10</sup>J. Noffke and L. Fritsche, *J. Phys. C* **14**, 89 (1981).
- <sup>11</sup>L. Gonzalez, R. Miranda, M. Salmerón, J. A. Vergés, and F. Ynduráin, *Phys. Rev. B* **24**, 3245 (1981).
- <sup>12</sup>R. Miranda, F. Ynduráin, D. Chandesris, J. Lecante, and Y. Petroff, *Phys. Rev. B* **25**, 527 (1982).
- <sup>13</sup>R. Miranda, F. Ynduráin, D. Chandesris, J. Lecante, and Y. Petroff, *Surf. Sci.* **117**, 319 (1982).
- <sup>14</sup>F. J. Himpsel and D. E. Eastman, *Phys. Rev. B* **21**, 3207 (1980).
- <sup>15</sup>U. Gradmann, K. Ullrich, J. Pebler, and K. Schmidt, *J. Magn. Mater.* **5**, 339 (1977).
- <sup>16</sup>J. C. Slater and G. F. Koster, *Phys. Rev.* **94**, 1498 (1954).
- <sup>17</sup>V. L. Moruzzi, J. F. Janak, and A. R. Williams, *Calculated Electronic Properties of Metals* (Pergamon, New York, 1978).
- <sup>18</sup>L. C. Davis and L. A. Feldkamp, *Solid State Commun.* **34**, 141 (1980).
- <sup>19</sup>A. Liebsch, *Phys. Rev. Lett.* **43**, 1431 (1979); *Phys. Rev. B* **23**, 5203 (1981).
- <sup>20</sup>C. Herring, in *Exchange Interactions among Itinerant Electrons*, Vol. IV of *Magnetism*, edited by G. T. Rado and H. Suhl (Academic, New York, 1966), and references therein.
- <sup>21</sup>C. Herring, in *Exchange Interactions among Itinerant Electrons*, Ref. 20, p. 227.
- <sup>22</sup>J. Friedel, in *Physics of Metals: I Electrons*, edited by J. M. Ziman (Cambridge University Press, Cambridge, 1969), p. 376.
- <sup>23</sup>J. Friedel and C. M. Sayers, *J. Phys. (Paris)* **38**, 697 (1977).
- <sup>24</sup>E. Merzbacher, *Quantum Mechanics*, 2nd ed. (Wiley, New York, 1970), p. 538.
- <sup>25</sup>*Handbook of Mathematical Functions*, edited by M. Abramowitz and I. Stegun (National Bureau of Standards, Washington, D.C., 1964).
- <sup>26</sup>C. S. Wang and A. J. Freeman, *Phys. Rev. B* **19**, 793 (1979).
- <sup>27</sup>D. E. Eastman, F. J. Himpsel, and J. A. Knapp, *Phys. Rev. Lett.* **40**, 1514 (1978); F. J. Himpsel, J. A. Knapp, and D. E. Eastman, *Phys. Rev. B* **19**, 2919 (1979).
- <sup>28</sup>W. Eberhardt and E. W. Plummer, *Phys. Rev. B* **21**, 3245 (1980).
- <sup>29</sup>J. A. Appelbaum and D. R. Hamann, *Solid State Commun.* **27**, 881 (1978).
- <sup>30</sup>F. Batallan, I. Rosenman, and C. B. Summers, *Phys. Rev. B* **11**, 545 (1975). The measured bulk magnetization of  $1.72\mu_B$  is believed to reflect a spin imbalance of  $n_{\uparrow} - n_{\downarrow} = 1.56$  electrons per atom with a  $g$  factor of approximately 2.2.
- <sup>31</sup>D. A. Shirley, in *Photoemission in Solids: I General Principles*, edited by M. Cardona and L. Ley (Springer, Berlin 1978), p. 165.
- <sup>32</sup>L. A. Feldkamp and L. C. Davis, *Phys. Rev. Lett.* **43**, 151 (1979).